Mesoscopic Fano effect in a quantum dot embedded in an Aharonov-Bohm ring

Kensuke Kobayashi, Hisashi Aikawa, Shingo Katsumoto, and Yasuhiro Iye
Institute for Solid State Physics, University of Tokyo, 5-1-5 Kashiwanoha, Chiba 277-8581, Japan
(Received 28 February 2003; revised manuscript received 10 July 2003; published 5 December 2003)

The Fano effect, which occurs through the quantum-mechanical cooperation between resonance and interference, can be observed in electron transport through a hybrid system of a quantum dot and an Aharonov-Bohm ring. While a clear correlation appears between the height of the Coulomb peak and the real asymmetric parameter q for the corresponding Fano line shape, we need to introduce a complex q to describe the variation of the line shape by the magnetic and electrostatic fields. The present analysis demonstrates that the Fano effect with complex asymmetric parameters provides a good probe to detect a quantum-mechanical phase of traversing electrons.

DOI: 10.1103/PhysRevB.68.235304 PACS number(s): 73.21.La, 85.35.−p, 73.23.Hk, 72.15.Qm

I. INTRODUCTION

An Aharonov-Bohm (AB) ring and a quantum dot (QD) have been typical mesoscopic systems that continually invoke fundamental interest in the researchers. The wave nature of electron manifests itself in the former while the particle nature of electron features in the latter. Combination of these complementary systems into a hybrid one enables us to explore the problem how coherent is the transport of electrons through a QD, where many electrons interact with each other. In 1995, Yacoby *et al.*[1] performed a pioneering work to tackle this issue by using such a system, namely, a QD embedded in one arm of an AB ring. It was found that an electron at least partially maintains its coherence in passing the QD.[1,2] As regards the phase of the AB oscillation, although phase lapse was found across the Coulomb peak, it was subsequently recognized to be due to the two-terminal nature of the device,[3,4] thus revealing that intrinsic phase measurement is a nontrivial issue. To avoid the problem, four-terminal measurements were performed and it was found that each level inside the QD acts as a Breit-Wigner-type scatterer in that the phase of electron smoothly changes π at the resonance.[5] At the same time, however, it has been found contrary to a naive expectation that the peaks in the Coulomb oscillations are in phase with each other and an unexpected phase lapse occurs at the middle of the Coulomb valley. Such an interferometry has also been applied to QD's in the Kondo regime,[6–8] while the results have not converged, again revealing the difficulty.[9]

In the above experiments, the transport properties of a QD have been the main scope and the other arm with no QD has served as ''reference.'' However, one might ask what happens if the coherence of the QD and the AB ring is fully maintained and thus the arm as well as the QD should be equally treated. In this situation, Fano effect has been expected to occur,[10–16] and was experimentally established in our previous study.[17]

Let us briefly summarize Fano theory.[18] Consider a system with a discrete energy state embedded in the continuum, which can be described by the following Hamiltonian [see Fig. 1(a)]:

$$\mathcal{H}=E_{\varphi}|\varphi\rangle\langle\varphi|+\sum_{E'}E'|\psi_{E'}\rangle\langle\psi_{E'}| + \sum_{E'}(V_{E'}|\psi_{E'}\rangle\langle\varphi|+V_{E'}^{*}|\varphi\rangle\langle\psi_{E'}|), \quad (1)$$

where φ is a discrete state with energy E_{φ} and $\psi_{E'}$ is a state in the continuum with energy E'. $V_{E'}$ is the coupling strength between the discrete state and the continuum. A system eigenstate Ψ_E can be expressed by a linear combination of φ and $\{\psi_{E'}\}$ with the coefficients analytically obtained. We consider a situation that an incoming initial state i interacts with the system through a perturbation $\mathcal{T}$ and ends up as a linear combination of $\{\Psi_E\}$. The evolution from i to Ψ_E consists of two paths: one is through continuum states and the other is through a ''resonant state'' Φ, which is a modi-

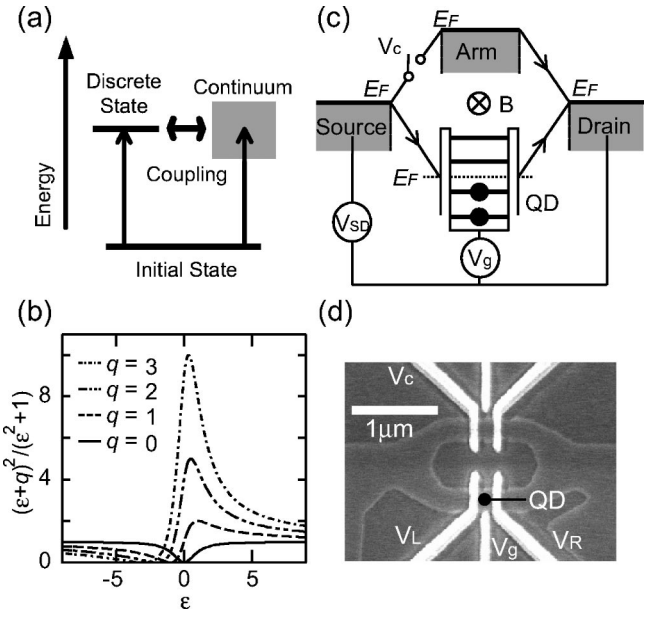

FIG. 1. (a) Principle of the Fano effect. (b) Fano's line shapes for several real q parameters. (c) Schematic representation of the experimental setup (see text). (d) Scanning electron micrograph of the correspondent device.

fication of φ through the interaction $V_{E'}$ with the continuum. The transition probability has a peculiar property around the resonance energy as

$$\frac{|\langle \Psi_E|\mathcal{T}|i\rangle|^2}{|\langle \psi_E|\mathcal{T}|i\rangle|^2}=\frac{(\epsilon+q)^2}{1+\epsilon^2} \quad \text{with} \quad \epsilon=\frac{E-E_0}{\Gamma/2}, \tag{2}$$

where E_0 and Γ are the energy position and width of the resonance state, respectively. The so-called ''Fano's asymmetric parameter'' q is defined as

$$q\equiv\frac{\langle \Phi|\mathcal{T}|i\rangle}{\pi V_E^*\langle \psi_E|\mathcal{T}|i\rangle}, \tag{3}$$

which is a measure of the coupling strength between the continuum state and the resonance state (namely, the strength of the configuration interaction). Several curves for different q's are plotted in Fig. 1(b).

The Fano effect is an expansion of the Breit-Wigner-type resonance scattering and was established in the atomic physics more than 40 years ago. Since then, reflecting the generality of the original model of Eq. (1), the Fano effect has been found ubiquitous in a large variety of experiments including neutron scattering,[19] atomic photoionization,[20] Raman scattering,[21] and optical absorption.[22] As this effect is essentially a single-impurity problem, an observation on a single site would reveal this phenomenon in a more transparent way. The most sensitive probe for such single-site experiments is the electron transport. Compared to its long history in the spectroscopy, however, the general importance of Fano effect in the transport was only recently pointed out in Refs. 23 and 24, although its characteristic feature has already appeared in the theoretical studies.[25] Experimentally, the single-site Fano effect has been reported in the scanning tunneling spectroscopy of an atom on the surface[26,27] and in transport through a QD.[28,29] While the latter case is the first observation of this effect in a mesoscopic system, there is no well-defined continuum energy state and the mechanism for the appearance of the effect remains as an intriguing puzzle.

As mentioned, the QD-AB-ring hybrid system with parameters appropriately tuned provides a unique Fano system where the transition process shown in Fig. 1(a) is realized in real space as schematically sketched in Fig. 1(c). An electron traverses from the source to the drain along two interfering paths. One is through the discrete state in the QD and the other is through the arm. In the previous paper[17] we reported the following: (i) The electronic states in the QD-AB-ring system can be sufficiently coherent for the Fano effect to emerge in transport. (ii) The coherent Fano state disappears at finite source-drain voltage. (iii) The phase difference between the two paths can be controlled by magnetic field, resulting in characteristic variation in the line shape of the resonant peaks, which suggests the necessity to treat the parameter q as a complex number.

Regarding this issue, many problems are still open. For instance, the phase controlling of the Fano effect should be clarified in terms of a complex q. In addition, we would list the phase evolution of the electrons through a QD in the presence of the Fano effect,[30,31] the Fano effect as a probe of phase coherence,[32] the Fano effect in the Kondo regime,[14] and the detailed mechanism for the zero-bias resonance peak/dip in the differential conductance through a Fano system.[17,28]

In this paper, after briefing the experimental setup in Sec. II, we extend the previous work to quantitative analysis of the experiments in Sec. III. First, we report the application of the conventional Fano formula with a real q to our observation, and discuss the relation between the original Coulomb peaks and the Fano peaks in Sec. III A. Then, we focus on the magnetic and electrostatic phase controlling of the Fano effect in Secs. III B and III C, respectively. This subject is the central part of this paper, where we show that Fano effect can be a powerful tool to investigate the electron phase variation in such mesoscopic transport. In Sec. III B, we actually derive complex q as a function of the magnetic field from the experiment and compare it with the theory. The electrostatic controlling of the Fano line shape is similarly analyzed in Sec. III C. We also discuss the phase evolution over multiple resonances and the temperature dependence of the Fano effect in Secs. III D and III E, respectively.

II. EXPERIMENT

Figure 1(d) shows a scanning electron micrograph of the device fabricated by wet-etching a two-dimensional electron gas (2DEG) in an AlGaAs/GaAs heterostructure (mobility $=9\times10^5$ cm^2/Vs and sheet carrier density $=3.8\times10^{11}$ cm^{-2}). The length of one arm of the ring L is ~2 μm. Two sets of three fingers are Au/Ti metallic gates to control the local electrostatic potentials of the device. The three gates (V_R, V_L, and V_g) at the lower arm are used for controlling the parameters of QD (with area about 0.15×0.15 μm^2) and the gate at the upper arm is to apply V_C, which determines the conductance of the upper arm. Measurements were performed in a mixing chamber of a dilution refrigerator between 30 mK and 800 mK by a standard lock-in technique in the two-terminal setup with an excitation voltage of 10 μV (80 Hz, 5 fW) between the source and the drain. Noise filters were inserted into every lead below 1 K as well as at room temperature.

As sketched in Fig. 1(c), this single-site Fano system is tunable in several ways. In the addition energy spectrum, the discrete energy levels inside the QD are separated by respective quantum confinement energy and the single-electron charging energy E_c, but we can shift the spectrum by the center gate voltage V_g to tune any one of them to the Fermi level. The coupling between the continuum and the levels in the QD is controlled by V_R and V_L. V_C can control the conductance of the interference path as well as the phase shift of the electrons traversing underneath it (details are given later). The controlling of the phase difference between the two paths ($\Delta\theta$) is also possible by the magnetic field B piercing the ring.

An advantage of the present sample structure (wrap-gate-type dot definition) is clearly shown in Fig. 2. The Coulomb oscillations through the QD with and without the conduction through the other arm show a clear one-to-one correspondence of the conductance peaks. This is due to the weakness

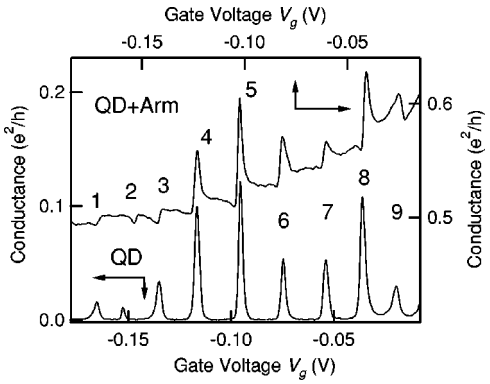

FIG. 2. Typical Coulomb oscillation at $V_C=-0.11$ V with the arm pinched off, and asymmetric Coulomb oscillation at $V_C=-0.085$ V with the arm transmissible. The latter shows a clear Fano effect. The Coulomb and Fano peaks are in good one-to-one correspondence as they were numbered consecutively from 1 to 9. Both of them were obtained at $T=30$ mK and $B=0.91$ T.

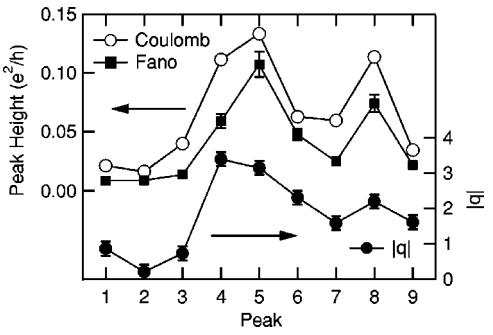

FIG. 3. Fitted q values for the peaks 1–9 in Fig. 2 are shown in the lower panel. The heights of Coulomb peaks and Fano peaks are also plotted in the upper panel. The three of them are well correlated.

in the electrostatic coupling between the two sets of gates (V_C and $\{V_L, V_g, V_R\}$), i.e., the circuit is already defined by etching and the gate electrodes can be very thin. Still, though, we need a small shift by 0.0065 V between the upper and lower axes in Fig. 2, due to the electrostatic coupling between the gates.

III. RESULTS AND DISCUSSION

A. Fano effect in the Coulomb oscillation

In Fig. 2, the peaks were numbered consecutively from 1 to 9. The small irregularity of the peak positions reflects the variation of single-electron energy-level spacing in the QD and indicates that the transport is through each single level. This is also consistent with the fact that the peak heights vary randomly. In the upper panel, the Fano effect emerges and the line shapes of the peaks become very asymmetric and even change to a dip structure for the peaks 1, 2, and 3.

We have found that the line shapes of the peaks in the upper curve in the conductance $G_{tot}(V_g)$ can be well fitted to the following equation:

$$G_{tot}(V_g)=G_{bg}+G_{Fano}(V_g), \tag{4}$$

where G_{bg} is noninterfering contribution of the parallel arm and is a smooth function of V_g that can be treated as a constant for each peak. G_{Fano} is the Fano contribution expressed as

$$G_{Fano}(V_g)=A\frac{(\epsilon+q)^2}{1+\epsilon^2} \quad \text{with} \quad \epsilon=\frac{\alpha(V_g-V_0)}{\Gamma/2}. \tag{5}$$

Here, A, V_0, and Γ are the amplitude, the position, and the width of the Fano resonance, respectively. α is the proportionality factor which relates the gate voltage V_g to the electrochemical potential of the QD. In our system, $\alpha \sim 20$ μeV/mV as estimated from the differential conductance at the finite source-drain voltages V_{sd}.[17]

The fitted values Γ are 40–60 μeV, reflecting the variation of the coupling strength between the leads and the QD in the original Coulomb peaks. This Γ is consistent with the width of the zero-bias peak observed in the differential conductance at a finite V_{sd}.[17] Figure 3 shows the fitted $|q|$ for the nine peaks. The signs of q are positive for all the peaks except the peak 9. This corresponds to the observation that all the Fano features (the dips 1–3 and peaks 4–8) except 9 have the asymmetric tails to the same direction. It is important that the signs of q are same for many consecutive Fano peaks since this directly reflects that the Coulomb peaks are in phase as introduced in Sec. I. We will discuss it in Sec. III D.

In the upper panel of Fig. 3, we plot the heights of the Coulomb peaks and the Fano peaks. The height of a Fano peak is defined as $A(1+q^2)$ in the fitting form of Eq. (5), which is the difference of the conductance maximum and minimum of the Fano resonance. Not only are the heights of the Coulomb and Fano peaks correlated but the observed $|q|$ values are also related to the peak heights in a way that a large peak tends to have a large $|q|$. This can be qualitatively explained as follows. When the arm is pinched off, electrons never pass the continuum, resulting in $|\langle\psi_E|\mathcal{T}|i\rangle|\to 0$. This corresponds to $|q|\to\infty$ in Eq. (3) and Eq. (2) asymptotically gives a Lorentzian Coulomb peak as seen in Fig. 1(b). This reflects the fact that the Fano theory includes the Breit-Wigner scattering problem as a special limit of $|q|\to\infty$, where there is no path through the continuum, namely, there is no configuration interaction. The height of the Coulomb peak is proportional to $|\langle\Phi|\mathcal{T}|i\rangle|^2$, which corresponds to the coupling strength between the QD and the leads. Opening of the arm means that $|\langle\psi_E|\mathcal{T}|i\rangle|$ is increased from 0 to a finite value with $|\langle\Phi|\mathcal{T}|i\rangle|$ fixed. The asymmetric parameter $|q|$, therefore, is larger for a larger original peak.

The above Fano effect was observed at $B\sim 0.91$ T. We found the Fano effect prominent within several specific magnetic-field ranges as shown in Figs. 4(a)–4(d) besides $B\sim 0.91$ T, while it was less pronounced in other ranges. This implies that the coherence of the transport through the QD strongly depends on B. A similar role of B is reported in the Kondo effect in a QD,[6] where the Kondo effect appeared at the specific magnetic field other than at $B\sim 0$ T. The phenomena arise from the change of the electronic states caused by B in a QD. It is also possible that the magnetic field

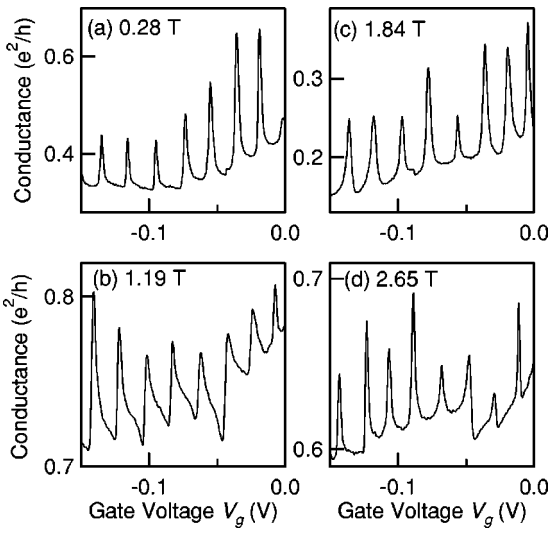

FIG. 4. Fano's line shapes taken at (a) 0.28 T, (b) 1.19 T, (c) 1.84 T, and (d) 2.65 T. They were obtained at $T=30$ mK.

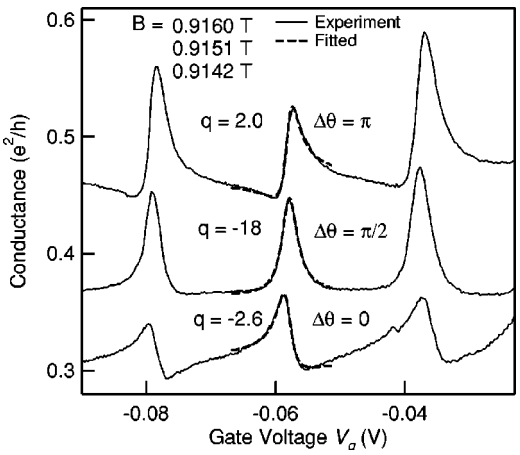

FIG. 5. Conductance of three Fano peaks at 30 mK at the selected magnetic fields at $B=0.9142$, 0.9151, and 0.9160 T. They are incrementally shifted upwards for clarity. The direction of the asymmetric tail changes between $B=0.9142$ and 0.9160 T, and the symmetric shape appears at 0.9151 T. The results of the fitting with Fano's line shape with real q's are superposed.

affects the coherent transport in the AB ring, due to the reduction of boundary roughness scattering by the magnetic field as theoretically treated in Ref. 33. An example of the experimental indication may be seen in Ref. 34. Henceforth, we will focus on the Fano effect observed at $B\sim 0.91$ T.

B. Magnetic-field control of the Fano interference

One of the experimental advantages of the present system over the other canonical Fano systems with microscopic sizes lies in the spatial separation between the discrete level and the continuum, which allows us to control Fano interference both magnetically and electrostatically.

The result of the magnetic controlling of the Fano effect was already reported (Fig. 4 of Ref. 17); Fano's asymmetric Coulomb oscillation appears in sweeping V_g at a fixed magnetic field, while the field sweeping at a fixed V_g results in the AB oscillation. Figure 5 shows the asymmetric oscillation obtained at $B=0.9142$, 0.9151, and 0.9160 T. Defining the first as $\Delta\theta=0$, the second and the third correspond to $\Delta\theta=\pi/2$ and π, respectively, as is calculated from the AB period ~ 3.6 mT. The peaks at $\Delta\theta=0$ and π are very asymmetric while those at $\Delta\theta=\pi/2$ are almost symmetric. The peaks at $V_g=-0.058$ V are fitted to Eq. (4) as indicated by the dashed curves. The obtained q's are -2.6, -18, and 2.0 for $\Delta\theta=0$, $\pi/2$, and π, respectively. This result is sufficient for one to cast doubts on the applicability of Eq. (5) with a real q. Since q serves as a measure for the strength of the configuration interaction, it is unphysical that q changes drastically and periodically by the small variation of the magnetic field. Treating q as a real number also conflicts the observation that the peaks become symmetric at specific fields, because Eq. (5) never gives a symmetric line shape for a real q unless $|q|\to\infty$ or $q=0$ and the divergence of q should be ruled out, which means that there is no configuration interaction.

To overcome these unphysical situations, we should take into account that the field only affects the phase of the electron and never changes the strength of the configuration interaction. In the original situation of the Fano theory,[18] this does not occur because the scattering center and the continuum are spatially overlapping. Hence q can be treated as a real number. Even in the framework of the Hamiltonian expressed in Eq. (1), this can be performed by treating V_E as a complex number and by assuming that the field only modifies $\arg(V_E)$ but not $|V_E|$. As a consequence, the generalized Fano formula is proposed in the following expression as an expansion of Eq. (5):

$$G_{Fano}(V_g,B)=A\frac{|\epsilon+q|^2}{\epsilon^2+1}=A\frac{(\epsilon+\mathrm{Re}q)^2+(\mathrm{Im}q)^2}{\epsilon^2+1}. \quad (6)$$

Qualitatively, even when the coupling strength $|q|$ is almost independent of B, the B dependence of $\arg(q)$ that comes from V_E in Eq. (3) yields asymmetric and symmetric line shapes of G for $|\mathrm{Re}q|\gg|\mathrm{Im}q|$ and $|\mathrm{Re}q|\ll|\mathrm{Im}q|$, respectively. We treated q as real in the analysis of the peaks in Fig. 2, which is justified as their asymmetry is large enough.

We note that q in Eq. (3) is not necessarily real. Conventionally q has been considered to be real, which is valid only when the system has the time-reversal symmetry (TRS) and thus the matrix elements defining q in Eq. (3) can be taken as real. This is the case in many experimental situations of microscopic Fano systems as far as their ground state has TRS, because it needs enormous magnetic field to add considerable AB phase during the transition between the continuum and the discrete states. Hence the breaking of TRS becomes important with enlargement of systems. The claim that Fano's asymmetric parameter q should be complex was theoretically considered in spectroscopy.[35–38] Also in the electron transport through mesoscopic systems, such generalization has been discussed or alluded.[13–16,32,39,40] To the best of our knowledge, though, our result is the first convincing experi-

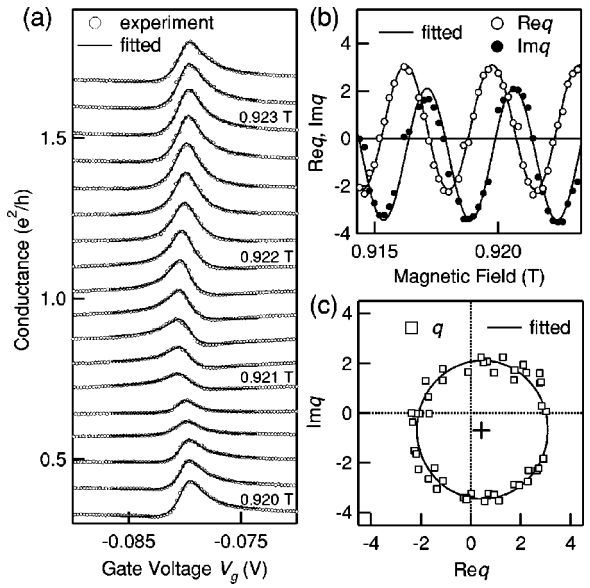

FIG. 6. (a) Conductance of the system measured at 30 mK at different magnetic fields that cover one AB period. The open circles and the solid curves are the experiments and the results of the fitting, respectively. They are incrementally shifted upwards for clarity. (b) Obtained Req and Imq are plotted. The solid curves are the fitted sinusoidal curves. (c) Result of (b) plotted in the complex q plane by treating B as an internal parameter. The cross indicates the ellipse center of the complex q.

mental indication that q should be a complex number, when TRS is broken under the magnetic field.

In order to be more quantitative, we carried out numerical fitting with complex q's to the line shape of the peaks occurring in the range $B=0.91$–0.93 T. The fitting function is Eq. (4) with Eq. (6) for $G_{Fano}(V_g)$, with Req, Imq, V_0, Γ, A, and G_{bg} as free parameters. The values of V_0 and Γ can be determined straightforwardly. As for the other four parameters, Req, Imq, A, and G_{bg}, the numerical fitting alone does not allow unique determination of all of them, because the functional form of Eq. (4) essentially contains only three parameters besides V_0 and Γ. We took the following fitting procedure. As has been argued in the discussion leading to Eq. (6), the amplitude A of the Fano resonance is expected to be nearly independent of B. Therefore, it is reasonable to assume that A takes a common value for all the curves to be fitted. The value of A was determined from the fitting of the most asymmetric case (since q can be taken as real) as $0.011e^2/h$, and this value was used for other curves. The resulting fitting is reasonably good over the whole range as shown by solid curves covering one AB period in Fig. 6(a). The V_0 and Γ are nearly independent of B, while the G_{bg} is found to change slightly with B due to the long tails of the neighboring Fano peaks.

In Fig. 6(b), the obtained Req and Imq are plotted against B. Both of them well depend on B sinusoidally, where the phase difference between the two sinusoids is very close to $\pi/2$. Indeed, the solid curves superposed on them are the result of the fitting by a sinusoidal function, that is, $\mathrm{Re}q(\Delta\theta)=0.4-2.6\cos(\Delta\theta)$ and $\mathrm{Im}q(\Delta\theta)=-0.7-2.7\times\sin(\Delta\theta)$. As defined above, $\Delta\theta$ is the phase difference picked up from the magnetic field based on the measured AB period, while $\Delta\theta=0$ corresponds to $B=0.9145$ T for these sinusoids.

The result is summarized as the plot of q in the complex plane shown in Fig. 6(c). The solid curve, which is elliptic (almost circular), is the result of the fitting in Fig. 6(b). As indicated by the cross, the ellipse center is slightly shifted from the origin $q=0$. The same fitting procedure for the other peaks at $V_g=-0.058$ V and -0.038 V in Fig. 5 yields complex q which also traces an ellipse with the center slightly shifted from the origin.

The generalized Fano formula for the two-terminal conductance of the QD-AB-ring system was theoretically proposed to be the same functional form with Eq. (6).[14,16] In the formula, the effect of the magnetic field is included in the phase factor $\Delta\theta$ in the complex q that is given as $q(\Delta\theta)=q_1\cos(\Delta\theta)+iq_2\sin(\Delta\theta)$. q_1, q_2, and A, which are real parameters independent of B, are defined by both the tunneling coupling between the QD and its leads and the coupling strength between the QD and the continuum energy state. The theoretical q traces an ellipse in the complex plane being consistent with our observation, while the theoretical ellipse center is at the origin. It is emphasized that this difference between the experiment and the theory is not caused by our fitting procedure. As is clear from Fig. 5, the heights of the peak at $V_g=-0.079$ V are different when the phase difference changes by π. This is also the case for the $V_g=-0.038$ V peak. These observations are never reproduced by using the theoretical form of $q(\Delta\theta)$, because, for an arbitrary $\Delta\theta$, the theoretical line shape for $q(\Delta\theta)$ is a mirror image of that for $q(\Delta\theta+\pi)$ with respect to $\epsilon=0$. Thus, the difference is due to the effect that is not included in the theoretical model. The influence of the multichannel transport and/or the orbital phase[41] might be a possible candidate. The incoherent transmission through the system may be also responsible for that, because q generally becomes complex due to the decoherence even under TRS.[32] As the present system is highly, but not perfectly, coherent, this would shift the ellipse center of the complex q from the origin.

C. Electrostatic control of the fano interference

Next, we focus on the electrostatic control of the Fano effect by the control gate voltage V_C. The variation of the electrostatic potential energy by V_C results in change in the kinetic energy of electrons, and hence their wave number which traverses the region underneath the gate electrode. As this gives rise to the phase difference between the path through the QD and the one through the arm,[42] the electrostatic controlling of the Fano effect is expected.

Figure 7(a) shows the asymmetric Coulomb oscillation at $V_C=-0.082$ V and -0.090 V. The direction of asymmetric tail of the Fano effect is opposite between the two. The result of the fitting to Eq. (4) with real q for the peak at $V_g=-0.102$ V is shown by the solid curve. In Fig. 7(b), the real q obtained for various V_C is plotted by the triangles. The

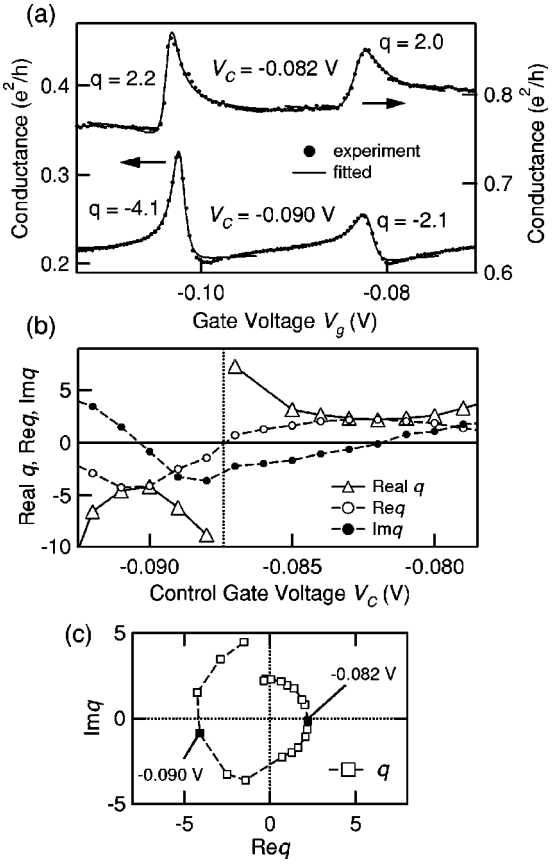

FIG. 7. (a) Coulomb oscillations at $V_C=-0.082$ V and -0.090 V at 30 mK and $B=0.91$ T. The results of the fitting to Eq. (4) are shown in the solid lines with the obtained q values. (b) Real q for the $V_g=-0.102$ V peak is plotted in the triangle as a function of V_C. The sign of q changes between $V_C=-0.088$ V and -0.087 V as indicated by the vertical dashed line. The obtained Req and Imq for the same peak are superposed with white and black circles, respectively. (c) Result of (b) plotted in the complex q plane by treating V_C as an internal parameter. q's for $V_C=-0.082$ V and -0.090 V are colored black.

line shape becomes symmetric with large $|q|$ at $V_C=-0.088$ V and -0.087 V, between which the sign of q changes.

The above behavior is similar to the one in the magnetic controlling. However, we note that there exists an essential difference between the magnetic controlling and the electrostatic one. While in the former a complex q is a natural consequence of the broken TRS, this is not the case in the latter because the electrostatic potential modulation itself never breaks TRS when the magnetic flux piercing the AB ring is integer times the flux quantum h/e. Nevertheless, when the flux is fixed to a noninteger value of flux quanta, a symmetric Lorentzian line shape can appear at specific V_C's and thus q should be complex. This can be proven in a model calculation by combining the Breit-Wigner formula with the conductance formula for the two-terminal AB ring[43] as performed in Ref. 13. Finite decoherence is also responsible for the occurrence of the symmetric line shape[32] as already discussed.

Figure 7(b) shows the result of the complex q for the various V_C's obtained by the similar fitting procedure as done in the magnetic controlling. As expected, both Req and Imq continuously change in sweeping V_C. Req crosses 0 with finite Imq between $V_C=-0.088$ V and -0.087 V while $|\mathrm{Re}q|$ takes its local maximum with Im$q\sim 0$ around $V_C=-0.082$ V and -0.090 V, where the line shape is the most asymmetric. So, the electrostatic controlling of the Fano effect can be characterized by the complex q as we have seen for the magnetic one. As we have discussed in Fig. 6(c), the result is summarized in Fig. 7(c) as the plot of q in the complex plane. Again, the complex q encircles around the origin of the complex plane.

Let us estimate the order of magnitude of the phase difference introduced by the change of V_C. According to a simple capacitance model between the gate and the 2DEG,[44,45] this effect yields the phase difference $\Delta\theta$;

$$\Delta\theta(V_C)=2\pi\frac{W}{\lambda_F}\left(1-\sqrt{1-\frac{V_C}{V_{dep}}}\right), \tag{7}$$

where W and V_{dep} are the width of the gate and the pinch-off voltage of the corresponding conduction channel (-0.10 V for the last channel in the present case), respectively. $\lambda_F\sim 40$ nm is the Fermi wavelength of the present 2DEG. Now, if we take the effective width $W\sim 120$ nm, $|\Delta\theta(V_C=-0.082)-\Delta\theta(V_C=-0.090)|=0.65\pi$ for the last and probably the most effective channel. Although this is expected to be π for the ideal case as seen from Fig. 7(c), the variation of the Fano line shape in Fig. 7(a) is attributed as due to such large phase difference electrostatically introduced by V_C.

We have seen that the electrostatic controlling of the Fano effect is possible. It is pointed out that this type of phase measurement is very difficult in ordinary oscillation of conductance.[42] A phase shift by π due to potential scattering means that the Fermi energy has passed a resonant energy level, which causes steep variation of the conductance by order of $2e^2/h$. Hence the oscillation due to the interference is almost swamped by in the large variation of the conductance. Indeed in the case of Fig. 7, the increase of the baseline for π phase shift is about $0.6e^2/h$ while the Fano asymmetry due to the interference is only about $0.02e^2/h$. Furthermore, V_{dep} in Eq. 7 is different for each conductance channel, meaning that the phase shift caused electrostatically is inevitably channel dependent. Hence the total conductance for the multichannel case is a superposition of many oscillations with various phase shifts.

The clear advantage of the present electrostatic tuning in overcoming the severe "signal-to-noise ratio" lies in the peculiar Fano line shape and in the insensitivity of the arm conductance to V_g. More importantly, the QD acts as a filter for the conductance channels, which means that in the Fano effect we selectively observe the interference through the single channel passing through the QD. The present result indicates that the analysis of the Fano resonance with Eq. 6 provides a sensitive and noise-resistant method to detect quantum-mechanical phase of electrons.

D. Phase evolution over multiple resonances

Thus far we have mainly focused on the transport in the small areas of the gate voltage around respective peaks. Here, we discuss the phase evolution of electrons between neighboring peaks. In Ref. 17, it has been reported that the phase changes by π rapidly but continuously across the resonance and that all the adjacent Fano resonances are in phase, as the phase makes another slow change by π between the valley. In contrast to the experiment for the phase measurement of the QD,[1] the present data not only reflect the phase evolution of electrons through a QD, but also represent the response to the magnetic field of the whole QD-AB-ring system. In that case, a continuous change by π at the resonance is likely.[16] What still remains surprising is the other gradual phase change by π at each valley.[46] This phenomenon is in clear contrast to the reported phase lapse in the middle of the valley,[5] which has not been perfectly understood yet despite extensive studies.[3,47–52] Nevertheless, in most cases, the adjacent Coulomb peaks are in phase. This is also consistent with our observation that the direction of the Fano asymmetry is usually the same in each curve as clearly seen in Figs. 2, 4(b), 5, and 7(a).

It should be added that in rare cases the adjacent peaks are in antiphase, as seen in the Fano peaks 8 and 9 in Fig. 2. This is the observation that has never been known before.[1,5] While the necessary condition for it remains to be clarified, this should be a new clue to the phase lapse problem.

E. Temperature dependence of the AB effect

The phase coherence over the system is essential in the controlling of the Fano interference discussed above. Figure 8(a) shows the temperature dependence of the Fano effect between 50 mK and 800 mK. While clear Fano features appear at 50 mK as marked by the arrows, they diminish rapidly as the temperature increases. Especially, the asymmetric dips at 50 mK evolves into peaks at $T \geqslant 200$ mK. While the thermal broadening of the Fano line shape is not negligible at temperatures higher than Γ,[29] it cannot explain such drastic temperature dependence. The main cause for this phenomenon is the decoherence induced by increasing the temperature, resulting in the destruction of the Fano state. This is confirmed by the temperature dependence of the AB effect. In Fig. 8(c), we plotted the AB amplitude at 50, 100, 200, 300, and 400 mK for the peak and the valley indicated in Fig. 8(b). At 50 mK, the AB amplitude is found to be comparable to the net peak height, indicating that the electronic states are highly coherent over the ring. At $T > 400$ mK, the AB amplitude was hardly visible. This is consistent with the observation in Fig. 8(a).

The AB amplitude monotonically decreases both at the peak and valley as shown in Fig. 8(c). Interestingly, it decays more slowly at the valley than at the peak. While the mechanism for such a temperature dependence is yet unclear, a logarithmic T dependence that might be reminiscent of the Kondo effect was reported for the Fano effect in a single QD.[28] On the other hand, the exponential-decay function of T was reported for the quasiballistic AB ring.[45,53–55] However, the observed temperature range Fig. 8(c) is not wide enough to distinguish these two dependencies.

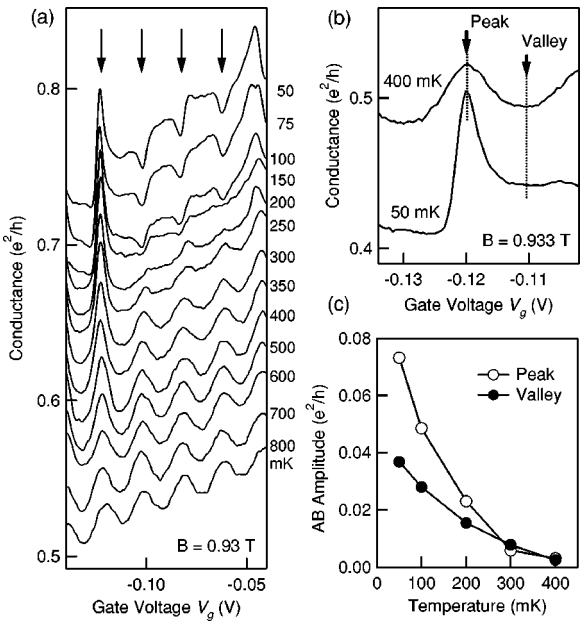

FIG. 8. (a) Conductance of the system measured between 50 mK and 800 mK at $B = 0.93$ T. The data at $T \leqslant 700$ mK are incrementally shifted upward for clarity. The Fano features marked by the arrows at 50 mK gradually disappear as the temperature increases. (b) Fano structure at 50 mK and 400 mK. (c) Temperature dependence of the AB amplitude measured at the peak and the valley indicated in (b).

IV. CONCLUSION

In summary, we have studied mesoscopic Fano effect observed in a QD-AB-ring system, especially in terms of the magnetic and the electrostatic tuning. In the conventional analysis with real q, the correlation between the original Coulomb peak heights and $|q|$ is observed. The magnetic-field tuning has revealed that the effect of TRS breaking can be taken into account by extending the Fano parameter q to a complex number. We have shown that the experimental curves can actually be fitted by adopting a complex q,[56] which shows slight systematic deviation from theoretical prediction. We have applied thus established method to the electrostatic tuning of Fano effect. This method clearly describes the electrostatic tuning of electron phase, which demonstrates that the Fano effect can be a powerful tool for phase measurement in mesoscopic circuits. Finally, we have reported the difference in the temperature dependence of the AB effect between the Coulomb peak and the Coulomb valley. Thus, we have clarified several aspects of the Fano effect observed in transport, while some problems remain to be solved in future such as the phase evolution over the multiple resonances.

It is interesting that the Fano effect first established in atomic physics is now observed in an artificial atom system. Such a mesoscopic analog will bring us renewed understandings. For example, the complex q should also be applied to other experiments where TRS is broken.

ACKNOWLEDGMENTS

We thank A. Aharony, M. Büttiker, O. Entin-Wohlman, M. Eto, W. Hofstetter, T.-S. Kim, J. König, and T. Nakanishi for helpful discussion. This work was supported by a Grant-in-Aid for Scientific Research and by a Grant-in-Aid for COE Research (''Quantum Dot and Its Application'') from the Ministry of Education, Culture, Sports, Science, and Technology of Japan. K.K. was supported by a Grant-in-Aid for Young Scientists (B) (Grant No. 14740186) from Japan Society for the Promotion of Science.

[1] A. Yacoby, M. Heiblum, D. Mahalu, and H. Shtrikman, Phys. Rev. Lett. **74**, 4047 (1995).
[2] S. Katsumoto and A. Endo, J. Phys. Soc. Jpn. **65**, 4086 (1996).
[3] A.L. Yeyati and M. Büttiker, Phys. Rev. B **52**, 14 360 (1995).
[4] A. Yacoby, R. Schuster, and M. Heiblum, Phys. Rev. B **53**, 9583 (1996).
[5] R. Schuster, E. Buks, M. Heiblum, D. Mahalu, V. Umansky, and H. Shtrikman, Nature (London) **385**, 417 (1997).
[6] W.G. van der Wiel, S. De Franceschi, T. Fujisawa, J.M. Elzerman, S. Tarucha, and L.P. Kouwenhoven, Science **289**, 2105 (2000).
[7] Y. Ji, M. Heiblum, D. Sprinzak, D. Mahalu, and H. Shtrikman, Science **290**, 779 (2000).
[8] Y. Ji, M. Heiblum, and H. Shtrikman, Phys. Rev. Lett. **88**, 076601 (2002).
[9] O. Entin-Wohlman, A. Aharony, Y. Imry, Y. Levinson, and A. Schiller, Phys. Rev. Lett. **88**, 166801 (2002).
[10] P. Singha Deo and A.M. Jayannavar, Mod. Phys. Lett. B **10**, 787 (1996); P. Singha Deo, Solid State Commun. **107**, 69 (1998).
[11] C.-M. Ryu and S.Y. Cho, Phys. Rev. B **58**, 3572 (1998).
[12] K. Kang, Phys. Rev. B **59**, 4608 (1999).
[13] O. Entin-Wohlman, A. Aharony, A., Y. Imry, and Y. Levinson, J. Low Temp. Phys. **126**, 1251 (2002).
[14] W. Hofstetter, J. König, and H. Schoeller, Phys. Rev. Lett. **87**, 156803 (2001).
[15] Tae-Suk Kim, Sam Young Cho, Chul Koo Kim, and Chang-Mo Ryu, Phys. Rev. B **65**, 245307 (2002).
[16] A. Ueda, I. Baba, K. Suzuki, and M. Eto, J. Phys. Soc. Jpn. **72**, Suppl. A, 157 (2003).
[17] K. Kobayashi, H. Aikawa, S. Katsumoto, and Y. Iye, Phys. Rev. Lett. **88**, 256806 (2002).
[18] U. Fano, Phys. Rev. **124**, 1866 (1961).
[19] R.K. Adair, C.K. Bockelman, and R.E. Peterson, Phys. Rev. **76**, 308 (1949).
[20] U. Fano and A. R. P. Rau, *Atomic Collisions and Spectra* (Academic Press, Orlando, 1986).
[21] F. Cerdeira, T.A. Fjeldly, and M. Cardona, Phys. Rev. B **8**, 4734 (1973).
[22] J. Faist, F. Capasso, C. Sirtori, K.W. West, and L.N. Pfeiffer, Nature (London) **390**, 589 (1997).
[23] E. Tekman and P.F. Bagwell, Phys. Rev. B **48**, 2553 (1993).
[24] J.U. Nöckel and A.D. Stone, Phys. Rev. B **50**, 17 415 (1994).
[25] For example, M. Büttiker, Y. Imry, and M.Ya. Azbel, Phys. Rev. A **30**, 1982 (1984); J.L. D'Amato, H.M. Pastawski, and J.F. Weisz, Phys. Rev. B **39**, 3554 (1989).
[26] V. Madhavan, W. Chen, T. Jamneala, M.F. Crommie, and N.S. Wingreen, Science **280**, 567 (1998).
[27] J. Li, W.D. Schneider, R. Berndt, and B. Delley, Phys. Rev. Lett. **80**, 2893 (1998).
[28] J. Göres, D. Goldhaber-Gordon, S. Heemeyer, M.A. Kastner, H. Shtrikman, D. Mahalu, and U. Meirav, Phys. Rev. B **62**, 2188 (2000).
[29] I.G. Zacharia, D. Goldhaber-Gordon, G. Granger, M.A. Kastner, Yu.B. Khavin, H. Shtrikman, D. Mahalu, and U. Meirav, Phys. Rev. B **64**, 155311 (2001).
[30] Amnon Aharony, Ora Entin-Wohlman, and Yoseph Imry, Phys. Rev. Lett. **90**, 156802 (2003).
[31] Tae-Suk Kim and S. Hershfield, Phys. Rev. B **67**, 235330 (2003).
[32] A.A. Clerk, X. Waintal, and P.W. Brouwer, Phys. Rev. Lett. **86**, 4636 (2001).
[33] H. Akera and T. Ando, Phys. Rev. B **43**, 11 676 (1991).
[34] L.P. Kouwenhoven, B.J. van Wees, W. Kool, C.J.P.M. Harmans, A.A.M. Staring, and C.T. Foxon, Phys. Rev. B **40**, 8083 (1989).
[35] G.S. Agarwal, S.L. Haan, and J. Cooper, Phys. Rev. A **29**, 2552 (1984).
[36] G. Abstreiter, M. Cardona, and A. Pinczuk, in *Light Scattering in Solids*, edited by M. Cardona and G. Güntherodt, Topics in Applied Physics Vol. 54 (Springer, Berlin, 1984), p. 127.
[37] K.J. Jin, S.H. Pan, and G.Z. Yang, Phys. Rev. B **50**, 8584 (1994).
[38] Wolfgang Ihra, Phys. Rev. A **66**, 020701 (2002).
[39] E.R. Racec and Ulrich Wulf, Phys. Rev. B **64**, 115318 (2001).
[40] Kicheon Kang and Sam Young Cho, cond-mat/0210009 (unpublished).
[41] Björn Kubala and Jürgen König, Phys. Rev. B **67**, 205303 (2003).
[42] S. Katsumoto, N. Sano, and S. Kobayashi, J. Phys. Soc. Jpn. **61**, 1153 (1992).
[43] Y. Gefen, Y. Imry, and M.Ya. Azbel, Phys. Rev. Lett. **52**, 129 (1984).
[44] A. Yacoby, U. Sivan, C.P. Umbach, and J.M. Hong, Phys. Rev. Lett. **66**, 1938 (1991).
[45] K. Kobayashi, H. Aiakwa, S. Katsumoto, and Y. Iye, J. Phys. Soc. Jpn. **71**, L2094 (2002).
[46] Since this feature is not included in Eq.(6), the fitting in Fig. 6(a) should be performed to the limited range of V_g around a single resonance, while the results of the fitting such as the behavior of the complex q are not greatly affected by a slight change of the fitting range.
[47] C. Bruder, R. Fazio, and H. Schoeller, Phys. Rev. Lett. **76**, 114 (1996).
[48] Y. Oreg and Y. Gefen, Phys. Rev. B **55**, 13 726 (1997).
[49] J. Wu, B.-L. Gu, H. Chen, W. Duan, and Y. Kawazoe, Phys. Rev. Lett. **80**, 1952 (1998).
[50] G. Hackenbroich and H. Weidenmüller, Europhys. Lett. **38**, 129 (1997).
[51] H.-W. Lee, Phys. Rev. Lett. **82**, 2358 (1999).
[52] T. Taniguchi and M. Büttiker, Phys. Rev. B **60**, 13 814 (1999).
[53] A.E. Hansen, A. Kristensen, S. Pedersen, C.B. Sørensen, and P.E. Lindelof, Phys. Rev. B **64**, 045327 (2001).
[54] G. Seelig and M. Büttiker, Phys. Rev. B **64**, 245313 (2001).
[55] G. Seelig, S. Pilgram, A. N. Jordan, and M. Büttiker, Phys. Rev. B **68**, 161310(R) (2003).
[56] The complex q was also reported recently in Jinhee Kim, Jae-Ryoung Kim, Jeong-O Lee, Jong Wan Park, Hye Mi So, Nam Kim, Kicheon Kang, Kyung-Hwa Yoo, and Ju-Jin Kim, Phys. Rev. Lett. **90**, 166403 (2003).